Cell, Volume *137*

Supplemental Data

Essential Role for TRPC5 in Amygdala Function and Fear-Related Behavior

Antonio Riccio, Yan Li, Jisook Moon, Kwang-Soo Kim, Kiersten S. Smith, Uwe Rudolph, Svetlana Gapon, Gui Lan Yao, Evgeny Tsvetkov, Scott J. Rodig, Ashlee Van't Veer, Edward G. Meloni, William A. Carlezon Jr., Vadim Y. Bolshakov, and David E. Clapham

SUPPLEMENTAL INTRODUCTION

In heterologous expression, homomeric channels formed by TRPC4 and TRPC5 exhibit an identical doubly rectifying current-voltage (I-V) relation (Schaefer et al., 2000; Strübing et al., 2001) due to voltage-dependent Mg^{2+} block at positive voltages (Obukhov and Nowycky, 2005). When coexpressed with TRPC1, they form heteromultimeric channels with a much smaller single channel conductance and exhibit a simpler whole-cell I-V relation. The heteromeric channel I-V has a gently negative slope at negative potentials and smooth outward rectification, reminiscent of NMDA receptor I-Vs (Strübing et al., 2001). Uniquely among TRP channels, TRPC4 and TRPC5 (and heteromers containing TRPC1) are potentiated by micromolar lanthanides (La^{3+} or Gd^{3+}) (Schaefer et al., 2000; Strübing et al., 2001), by interacting with an extracellular Ca^{2+}-binding site (Jung et al., 2003).

Supplemental References

Jung, S., Muhle, A., Schaefer, M., Strotmann, R., Schultz, G., and Plant, T. D. (2003). Lanthanides potentiate TRPC5 currents by an action at extracellular sites close to the pore mouth. J Biol Chem *278*, 3562-3571.

Obukhov, A. G., and Nowycky, M. C. (2005). A cytosolic residue mediates Mg^{2+} block and regulates inward current amplitude of a transient receptor potential channel. J Neurosci *25*, 1234-1239.

Schaefer, M., Plant, T. D., Obukhov, A. G., Hofmann, T., Gudermann, T., and Schultz, G. (2000). Receptor-mediated regulation of the nonselective cation channels TRPC4 and TRPC5. J Biol Chem *275*, 17517-17526.

Strübing, C., Krapivinsky, G., Krapivinsky, L., and Clapham, D. E. (2001). TRPC1 and TRPC5 form a novel cation channel in mammalian brain. Neuron *29*, 645-655.

SUPPLEMENTAL EXPERIMENTAL PROCEDURES

TRPC5$^{-/-}$ targeting construct. The targeting construct was linearized and electroporated into ES cells derived from 129/SvJ1 mice. G418-resistant colonies were selected and expanded. Southern blot using probes flanking the targeting construct sequence detected clones with successful homologous recombination. ES cells harboring the targeting construct were transfected with pOG231, a plasmid for transient Cre expression, to excise the neomycin cassette and create the conditional KO allele. Subsequent subclones were analyzed by genotyping those that underwent the appropriate recombination of loxP sites. Mice were treated in accordance with guidelines approved by the Children's Hospital Animal Care and Use Committee.

PCR analysis of mouse tail DNA. DNA was isolated from mouse tails according to standard protocols. A set of 3 primers was designed for genotyping. The primers: F1 was upstream of the first loxP site, R2 was located at the beginning of TRPC5 intron 5, R3 was located downstream of the second loxP site. The F1 and R2 amplified primers were designed to yield a 567 bp PCR fragment from wt *mTRPC5* gene; the F1 and R3 primers amplified a 693 bp PCR fragment from the disrupted targeted *TRPC5* gene.

Primer sequences were: F1, 5'-gtaagtgatactaggtatggggtatggagg-3'; R2, 5'-gaatatgatcggaattgggctgc-3'; and R3, 5'-gtcgacacacgtataaggcatactcttg-3'.

RT-PCR analysis. One µg was used to generate first-strand cDNA (Superscript III, Invitrogen). The KOF and KOR primers, spanning exon 4 to exon 7, amplified fragments of 436 bp and 296 bp from wt and *TRPC5*$^{-/-}$ cDNAs, respectively. Primer sequences: KOF, 5'-gtttcctatgctgtccatagcctatctg-3'; and KOR, 5'- ggatattgcgaagagtgcttctgc-3'.

In situ **hybridization.** Slides were incubated with anti-Digoxigenin-AP antibody overnight followed by nitroblue tetrazolium (NBT 340 µg/ml) and 5-bromo-4-chloro-3-indolyl phosphate (BCIP, 170 µg/ml) for 40 min in the dark. Color development was stopped, and the sections were placed on coverslips in buffered 50% glycerol. The mouse TRPC5-mRNA specific antisense riboprobe was directed against nucleotides 3752–4101 of the mTRPC5 sequence. Control experiments with sense probe did not label brain sections.

Immunoprecipitation and Immunohistochemistry IP buffer contained 20 mM HEPES–NaOH (pH 7.5), 1% Triton X-100, 150 mM NaCl, and protease inhibitors. For immunohistochemistry, slides were soaked in xylene, passed through graded alcohols, and placed in distilled water. Slides were then pre-treated with 10 mM citrate, pH 6.0 (Zymed) in a steam pressure cooker (Decloaking Chamber, BioCare Medical), followed by washing in distilled water. All subsequent steps were carried out at room temperature in a hydrated chamber. Slides were pre-treated with Peroxidase Block (DAKO USA) for

5 min to quench endogenous peroxidase activity. Slides were then washed in 50-mM Tris-Cl, pH 7.4, and incubated in Background Sniper (Biocare) for 10 min to reduce nonspecific background staining. Primary antibody cocktails consisted of either rabbit monoclonal antibody to CaMKIIα (1:1000; clone EP1829Y, Abcam,), rabbit polyclonal antibody to GFAP (1:2000; Abcam) or rabbit polyclonal antibody to Gad67 (1:100; AnaSpec) combined with mouse monoclonal to TRPC5 (1:500; clone: N67/15, NeuroMab, Davis, CA) and diluted in DaVinci Green diluent (Biocare) applied for 1 h. For double labeling, a cocktail of secondary antibodies (Alexa 555-conjugated goat anti-rabbit diluted 1:200, Molecular Probes, plus Envision anti-mouse, DAKO) was applied for 30 min. After washing, Cy5-tyramide Signal Amplification System (Perkin-Elmer Life Science Products) was applied in order to couple Cy5 dyes to the horseradish peroxidase-conjugated Envision secondary antibodies. Coverslips were sealed to slides with Prolong Gold Antifade Reagent with DAPI (Molecular Probes) to visualize nuclei. Slides were scanned on a PM2000 Imaging System (HistoRx) with SpotGrabber software (HistoRx), and exported through AQUA analysis software (HistoRx).

Behavioral assays

Elevated-plus maze

Mice were tested in a 110 x 110 x 85 cm black plastic maze (Hamilton Kinder, LLC), consisting of a center platform with four arms placed ~40 cm above the floor. Two of these arms were enclosed; the other two were open. Each arm of the maze was 10 x 50 cm; the intersection was 10 x 10 cm. Mice were allowed to acclimate to the dimly lit testing room (illuminated by a red 25 watt incandescent bulb) 1 h before testing. At the

time of testing, each mouse was placed in the center of the maze facing the same closed arm and videotaped for 5 min. An investigator blind to mouse genotype later scored videotapes. Open and closed arm entries and maze crosses were each quantified (control mice, n = 10; -/-, n = 10). Arm entry or exit was recorded when all four of the mouse's paws had entered or exited an arm.

Acoustic startle

Responses to loud sounds (acoustic startle) were measured in acoustic startle cages. Mice were placed in a 9 x 7 x 7 cm Plexiglas cage and attached to a load-cell platform. Both the startle cages and platform were contained within a 69 x 36 x 42 cm ventilated sound-attenuating isolation box. Temperature was maintained at ~20^{o}C. Startle amplitude was proportional to the amount of cage movement and defined as the maximum peak-to-peak voltage that occurred during the first 200 ms after the onset of the startle stimulus. After a 5 min acclimation period, 2 habituating startle stimuli (100 dB, 30 s interstimulus interval [ISI]) were given. Mice were then presented with 90 startle stimuli at each of 3 intensities (95, 100 and 105 dB) in a semi random order, at 30 s intervals (ISI; control mice, n = 10; knockout mice, n = 9). Activity was sampled in the 200 ms immediately preceding the onset of the startle stimuli. Startle amplitude data were expressed as the mean averaged across the different startle-eliciting intensities and as the average across all startle intensities. Activity data were expressed as the mean averaged across all trials.

Single-trial fear conditioning

On the training day, the mouse (wild-type or mutant) was placed in the conditioning chamber for 2 min before the onset of the conditioned stimulus (CS), a tone that lasted

for 30 s at 2800 Hz at 85 dB (Shumyatsky et al., 2002; 2005). The last 2 s of the CS were paired with the unconditioned stimulus (US), 0.7 mA of continuous foot shock. After an additional 30 s in the chamber, the mouse was returned to its home cage. Mice were tested at 30 min after training and at 24 hr after training. For testing, mice were placed in a novel environment (cage) in which the tone (120 s) that had been presented during training was given after a 1 min habituation period (control mice, n = 10; knockout mice, n = 10). Freezing scores were calculated as the fraction (percentage) of the total CS duration the mouse remained immobile (frozen).

Conditioned freezing following multiple CS-US pairings

Training and testing of animals was conducted in cages identical to those described above for measuring the acoustic startle response. The auditory conditioned stimulus (CS) was a 12 kHz (70 dB) tone delivered through a super-tweeter speaker located directly behind the startle cage. The unconditioned stimulus (US) was a shock delivered to the floor bars of each cage by a shocker/scrambler module. On Day 1, mice were placed in the startle cages and after a 5 min acclimation period, received 10 presentations of a 10 s tone (3 s rise time) co-terminating with a 0.5 ms, 0.4 mA shock (control mice, n = 10; null mice, n = 9). The mean intertrial interval was 3 min (range of 2-4 min). On Day 2 (24 h after training), mice were placed in the startle cages and after a 5-min acclimation period, presented with 20 trials; 10 trials of tone presentation and 10 trials with no tone presentation. All trials were presented in alternating order with a 30 s interstimulus interval. Cage movement was sampled every 10 ms during the 10 s tone presentation, or at an equivalent time in no-tone trials, and the sum of the integrated response was calculated for each trial. ‘Freezing’ behavior was measured as

the inhibition of activity during tone trials compared with no-tone trials, and calculated as a percent freezing score averaged across the 2 different trial types: % freezing = (activity-no-tone minus activity-tone)/ activity-no-tone.

Locomotor Activity

Mice were tested for up to 30 min after being placed in a polycarbonate cage (43 cm x 20 cm x 20 cm) transected by a horizontal infrared beam grid (4 x 8 cm) and surrounded by photobeam detectors (control mice, n = 8; null mice, n = 8). Horizontal and vertical photobeam breaks were recorded as a measure of locomotor activity. At the end of the trial mice were returned to the home cage. Locomotor activity, defined as consecutive breaking of photobeams, was recorded at 5 min intervals after a 1 h habituation period.

Open Field Testing

The open-field consisted of a white arena (40 cm × 40 cm × 40 cm) monitored by an automated video tracking system. The center area was illuminated by a 50 W halogen bulb (positioned 30 cm above field). Mice were placed in the periphery of the arena; the distance run and speed were recorded over a 12 × 5 min (1h) period (control mice, n = 8; null mice, n = 8). For further analysis, the following parameters were automatically calculated: total time spent in the central zone, number of entries into the zone, time of motor activity, and distance moved. Statistical analysis was conducted using the Statistical Analysis System (Version 9.1; SAS institute). Performance measures were analyzed using the PROC GLIMMIX program, a generalized linear mixed models procedure for conducting repeated measures analyses of non-normal data. Means were calculated for each animal for each testing condition.

Social interaction test

The apparatus used in this study and the testing procedures were the same as in McNaughton et al. (2008). Following habituation, testing was completed in a single session lasting 30 min. The testing session was comprised of 3 consecutive stages, including rehabituation (10-min duration), sociability phase (10-min duration) and preference for social novelty phase (10-min duration). At the start of the sociability phase, an unfamiliar male mouse was placed into one of the two small wire enclosures in the apparatus and the other wire enclosure in the opposite chamber was left empty. Left or right location was counterbalanced across the two experimental groups of mice. The experimental mouse was allowed to explore the entire apparatus for 10 min. To test the preference for social novelty, a second novel mouse was introduced into the wire enclosure on the opposite side of the apparatus. The stimulus mouse that had been present during the “sociability” phase is referred to as the “familiar” mouse and the newly introduced mouse is referred to as the “novel” mouse. The experimental mouse was subsequently allowed to freely explore the apparatus for 10 min. For behavioral analysis, the apparatus was divided into 18 identical squares. The apparatus consisted of 3 different areas: (1) The 4 squares immediately adjacent to the wire cage enclosing the familiar stimulus mouse, (2) the corresponding 4 squares immediately adjacent to the wire cage enclosing the socially novel mouse, and (3) the 10 squares that comprised the rest of the apparatus, termed the “non-cage” area. The duration of time spent in each area by control and TRPC5 null mice was measured (control mice, n = 7; null mice, n = 7). In the social novelty phase, the relative novelty preference score for the number of nose contacts with the two stimulus mice was defined as the difference in

the number of nose contacts a test mouse performed with the novel mouse and the familiar mouse.

Novelty-suppressed feeding

The novelty-suppressed feeding test was conducted as previously described (Santarelli et al., 2003). The apparatus was a clear Plexiglas box (40 x 40 cm x 31 cm), lined with 2-3 cm of clean bedding, illuminated by overhead lighting (20 lux), and surrounded on 3 sides by an opaque curtain. An inverted, clear plastic petri dish (100 x 20 mm; Becton Dickinson) lined with white paper was placed directly in the center of the apparatus onto which a single, clean food pellet (~4 g) was placed. Subjects were deprived of food (with *ad libitum* access to water) for 24 h (control mice, n = 10; null mice, n = 10). On the day of testing, subjects were removed from their home cage, placed into a holding cage for 60 min, and then placed into a corner of the testing apparatus. The latency to contact the pellet, the latency to bite the pellet, and the latency to begin eating the pellet were recorded (maximum test time = 6 min). Immediately after subjects began eating, they were removed from the test apparatus and returned to their home cage where they were allowed *ad libitum* access to a pre-weighed food pellet for 5 min. The latency to begin eating in the home cage and total food consumption were also measured.

Supplemental References

McNaughton, C.H., Moon, J., Strawderman, M.S., Maclean, K.N., Evans, J., and Strupp, B.J. (2008). Evidence for social anxiety and impaired social cognition in a mouse model of fragile X syndrome. Behav Neurosci *2*, 293-300.

Santarelli, L., Saxe M., Gross, C., Surget, A., Battaglia, F., Dulawa, S., Weisstaub, N., Lee, J., Duman, R., Arancio, O., *et al*. (2003). Requirement of hippocampal neurogenesis for the behavioral effects of antidepressants. Science *301*, 805-809.

SUPPLEMENTAL FIGURE LEGENDS

Figure S1. Expression of TRPC5 in auditory cortex. (A) Immunohistochemical analysis of the auditory cortex shows colocalization of cells expressing TRPC5 (left) and CaMKIIα (middle), a marker of pyramidal neurons (right). Scale bar, 25 μm.

Figure S2. TRPC5 was not detected in glial cells and interneurons. (A, B) Images indicate brain areas shown in C-E. **(C, D)** Immunohistochemical analysis shows that cells expressing TRPC5 (red) and GFAP (green; a marker of glial cells) do not co-localize in the auditory cortex (C) and the lateral nucleus of the amygdala (LA) (D), respectively. Scale bar, 50 μm. **(E, F)** Cells expressing TRPC5 (red) and GAD67 (green; a marker of interneurons) do not co-localize in the auditory cortex **(E)** and the lateral nucleus of the amygdala **(F)**. Scale bar, 50 μm.

Figure S3. Generation and verification of TRPC5-deficient mice. (A) Targeting strategy for the disruption of the *TRPC5* gene. Following homologous recombination, the deletion of exon 5 region was catalyzed by Cre-recombinase in ES cells. **(B)** PCR analysis of tail genomic DNA confirms targeting of the TRPC5 locus. **(C)** RT-PCR analysis using total RNA extracted from the whole brain of control and $TRPC5^{-/-}$ littermates confirms the absence of exon 5. **(D)** Immunoprecipitation analysis of TRPC5 protein in brain microsomes extracted from control and *TRPC5* knockout littermates reveals loss of TRPC5 protein in $TRPC5^{-/-}$ mice (upper panel). Western blotting of Na^+-K^+-ATPase confirms equal protein loading in control and $TRPC5^{-/-}$ littermates (lower

panel). **(E)** Immunohistochemical staining of CA1 and dentate gyrus from control and -/- littermates reveals selective loss of TRPC5 expression in null mice.

Figure S4. Quantitative RT-PCR determination of TRPC mRNA levels in mouse brain. (**A-E**) In whole brain, the mRNA levels of TRPC1, TRPC3, TRPC4, TRPC6 and TRPC7 were not significantly different between control and *TRPC5*$^{-/-}$ littermates. Data presented as mean ± SEM.

Figure S5. Conditioned freezing after multiple CS-US pairings and the novelty suppressed feeding in *wt* and *TRPC5*$^{-/-}$ mice. (A) Conditioned 'freezing' was enhanced in *TRPC5*$^{-/-}$ mice (n = 9) compared to littermate control mice (n = 10) at 24 h post-training following 10 CS-US pairings; $t_{(17)}$=2.26, P<0.05. **(B- E)** Novelty-suppressed feeding test in control and *TRPC5* null mice. There were no differences between groups (10 mice each group) in the latency to first contact the food pellet (**B,** t test, P = 0.69), latency to bite the pellet (**C,** P = 0.22), latency to begin eating the pellet (**D,** P = 0.25), and the amount of food eaten in the home cage (**E**, P = 0.50). Data are presented as mean ± SEM.

Figure S6. Quantitative RT-PCR determination of TRPC5, TRPC1, and TRPC4 mRNA levels in amygdala. (A) TRPC5-mRNA expression in amygdala of 5-week old control mice decreases to ~50% of that measured in 15-day old control mice. **(B, C)** TRPC1-mRNA and TRPC4-mRNA levels are not significantly different between control

and *TRPC5*$^{-/-}$ littermates. **(D)** Sequences of the oligonucleotides used for the quantitative RT-PCR. All data are presented as mean ± SEM.

Figure S7. Basal synaptic transmission in the cortico-amygdala pathway in 10-13 day-old *TRPC5*$^{-/-}$ mice. (A) Examples of cortico-amygdala EPSCs evoked by stimulation pulses of increasing intensity recorded in slices from control and *TRPC5*$^{-/-}$ mice. **(B)** Synaptic input-output curves obtained in slices from control or *TRPC5*$^{-/-}$ mice. Cortico-amygdala EPSCs were evoked under voltage-clamp (holding potential = – 70 mV) by electrical stimulation of fibers in the external capsule (cortical input to the LA). The intensity of stimulation was gradually increased from the threshold stimulus (determined for each individual experiment), in increments of 25 μA to produce EPSCs of increasing amplitude. The EPSC amplitude is plotted as a function of stimulation intensity. From 4 wt mice, n = 16 cells and 4 control mice, n = 21 cells. ANOVA, $P<0.04$. **(C)** Examples of paired-pulse facilitation of cortico-amygdala EPSCs in slices from control and mutant mice. The interstimulus interval was 50 ms. Traces are averages of 10 EPSCs. **(D)** Summary plot of the paired-pulse facilitation experiments. From 4 wt mice, n = 17 cells and 4 null mice, n = 22 cells. **(E)** Examples of mEPSCs recorded in neurons in the LA in slices from control and *TRPC5*$^{-/-}$ mice at –70 mV. **(F)** Cumulative amplitude (left) and inter-event interval (right) histograms of mEPSCs recorded in slices from control (open symbols) or *TRPC5*$^{-/-}$ (filled symbols) mice. **(G)** Summary plots of averaged values of mEPSC parameters; mean peak amplitude (*wt*: 9.2 ± 0.5 pA, 17 neurons from 4 *wt* mice and *TRPC5*$^{-/-}$: 8.4 ± 0.38 pA; 22 neurons from 4 null mice; t test, $P = 0.23$), and frequency (*wt*: 2.5 ± 0.44 Hz average of 17 neurons from 4 *wt* mice,

versus *TRPC5*$^{-/-}$: 3.15 ± 0.5 Hz average of 22 neurons from 4 null mice; t-test, *P* = 0.36; Error bars ± SEM.

Figure S8. Post-tetanic potentiation at the thalamo-amygdala synapses is normal in *TRPC5*$^{-/-}$ mice. Summary graphs of PTP experiments in slices from control and *TRPC5* null mice. The EPSCs were evoked at a holding potential of – 70 mV with 5-s interstimulus interval. PTP was induced by a 1-s train of 100-Hz stimulation (at arrow) in the presence of 50 μM D-APV in the bath solution. Traces show the average of 6 consecutive EPSCs recorded in individual experiments before and immediately after the 100-Hz stimulation in slices from control (left) and TRPC5$^{-/-}$ (right) mice. From 4 *wt* mice, n = 12 neurons and 4 *TRPC5* null mice, n = 8 neurons. *P* = 0.61; Error bars, ± SEM.

Figure S9. Summary box plots of asynchronous EPSC amplitude in cortical and thalamic inputs in slices from control and *TRPC5*$^{-/-}$ mice. The line inside the boxes marks the median, and the box boundaries indicate the 25th and 75th percentiles. The error bars indicate the 10th and 90th percentiles. Cortical input: from 3 *wt* mice, n = 11 neurons and 4 *TRPC5* null mice, n = 17 neurons, t-test, *P* = 0.27. Thalamic input: from 3 *wt* mice, n = 11 neurons and 4 *TRPC5* null mice, n = 16 neurons; t-test, *P* = 0.3.

Figure S10. Basal synaptic transmission in inputs to intercalated cells is normal in *TRPC5*$^{-/-}$ Mice. (A) Synaptic input-output curves for inputs from the LA to intercalated cells in slices from control or *TRPC5*$^{-/-}$ mice. The EPSCs in intercalated cells were

recorded under voltage-clamp conditions at a holding potential of –70 mV and evoked by the stimulation electrode placed in the LA. The EPSC amplitude is plotted as a function of stimulation intensity. The intensity of stimulation was gradually increased from the threshold stimulus, determined in each individual experiment, with an increment of 25 μA. Insets show the superimposed averages of 8 EPSCs evoked by weak and strong stimulation pulses in slices from both groups of mice. From 4 *wt* mice, n = 12 neurons and 4 *TRPC5* null mice, n = 11 neurons; ANOVA, *P*=0.58. **(B)** Summary plot of the paired-pulse facilitation experiments in intercalated cells. From 4 *wt* mice, n = 16 cells and 4 *TRPC5* null mice, n = 15 cells; t-test, *P*=0.47. The inter-stimulus interval was 50 ms. **(C)** Examples of sEPSCs recorded in intercalated cells in slices from control and *TRPC5*$^{-/-}$ mice at –70 mV. **(D)** Summary plots of averaged values of sEPSC parameters, mean peak amplitude (left t-test, *P* = 0.66) and frequency (right, t-test, *P* = 0.22), in control and TRPC5$^{-/-}$ mice. From 4 *wt* mice, n = 15 neurons and 4 *TRPC5*$^{-/-}$ mice, n = 14 neurons. Error bars, ± SEM.

SUPPLEMENTAL FIGURES

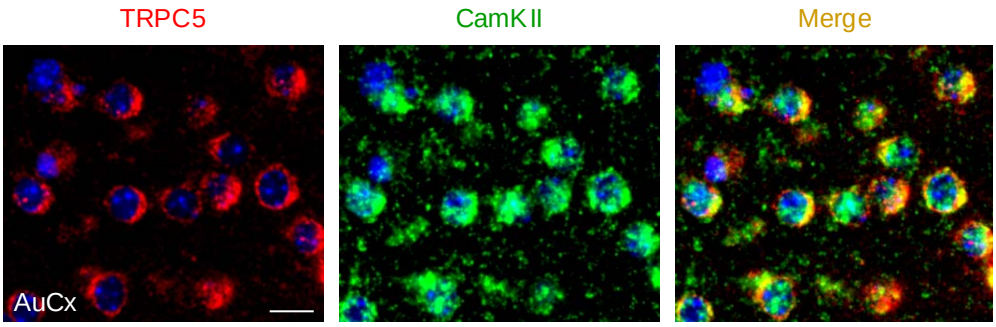

Supplementary Fig. 1
Riccio et al.

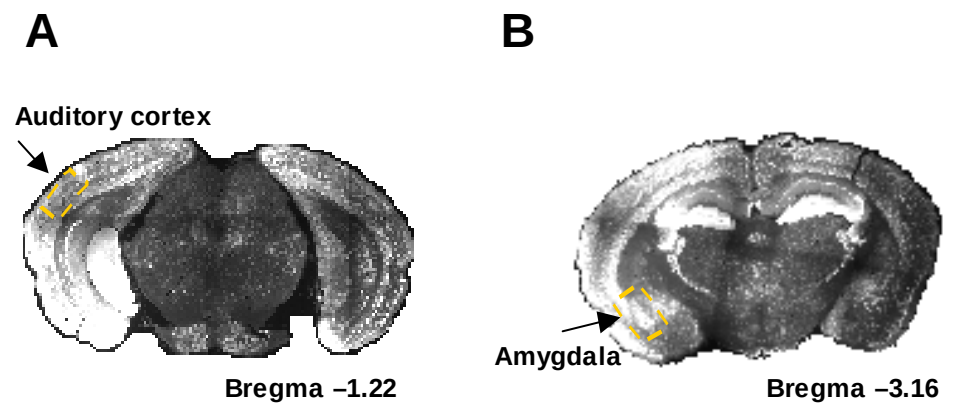

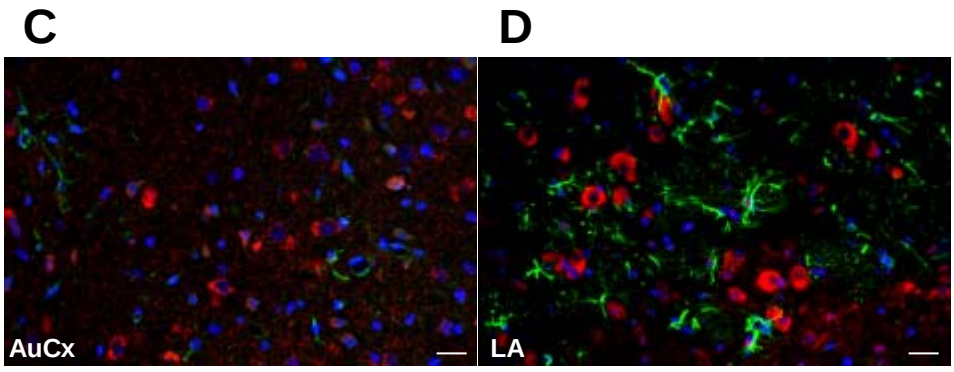

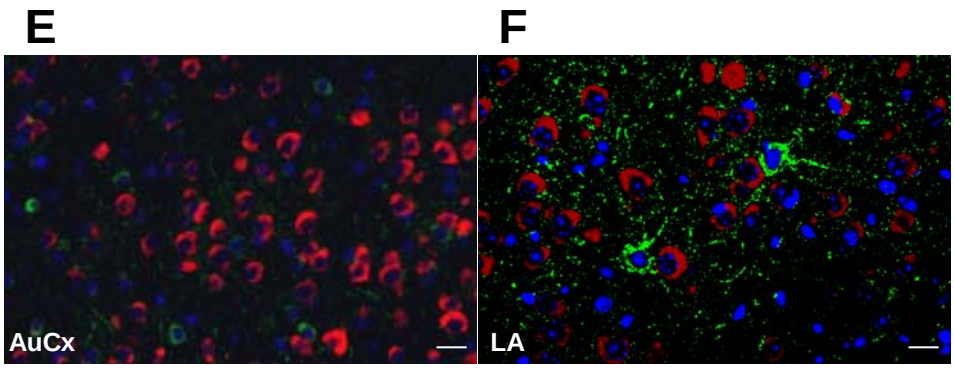

Supplementary Fig. 2
Riccio et al.

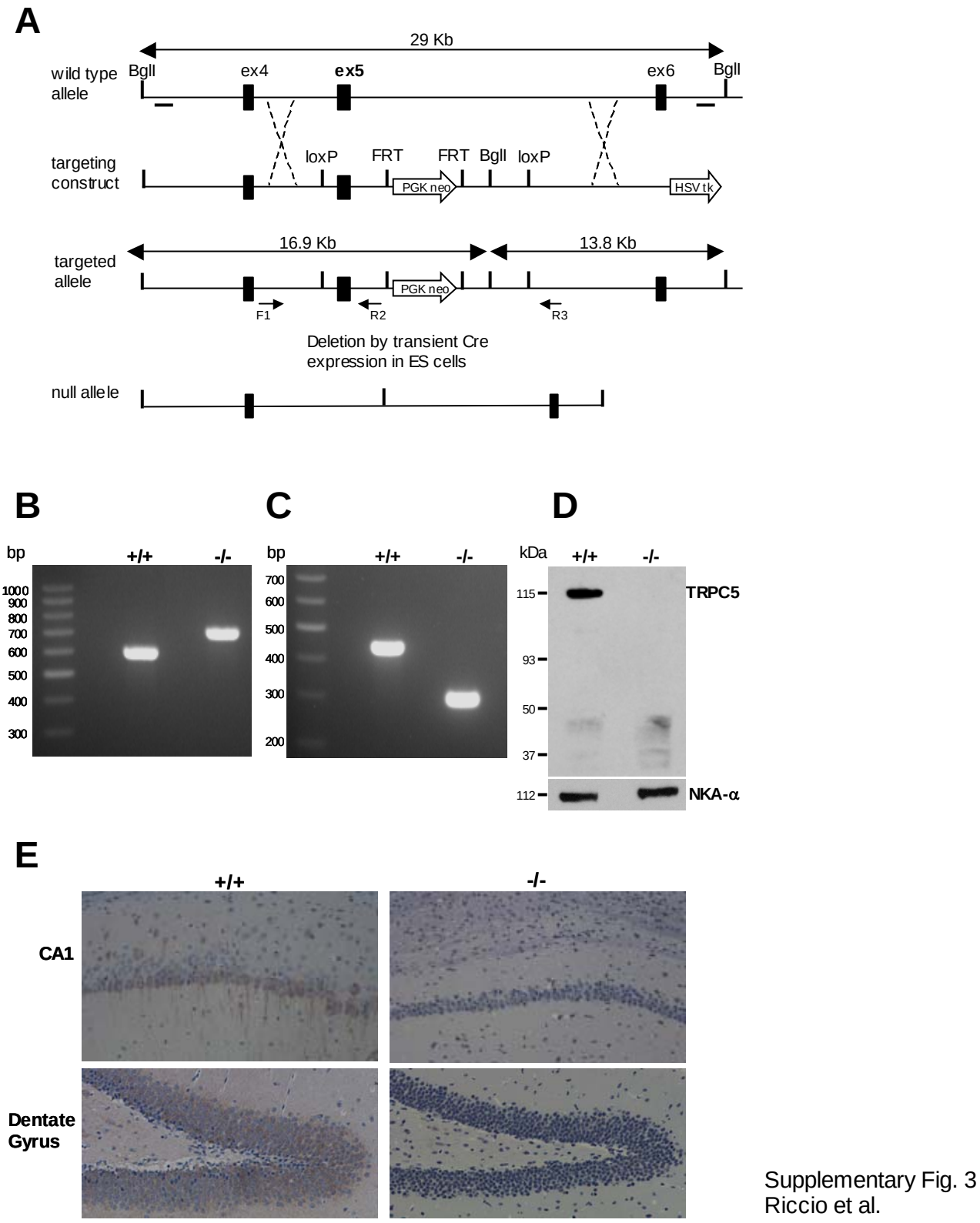

Supplementary Fig. 3
Riccio et al.

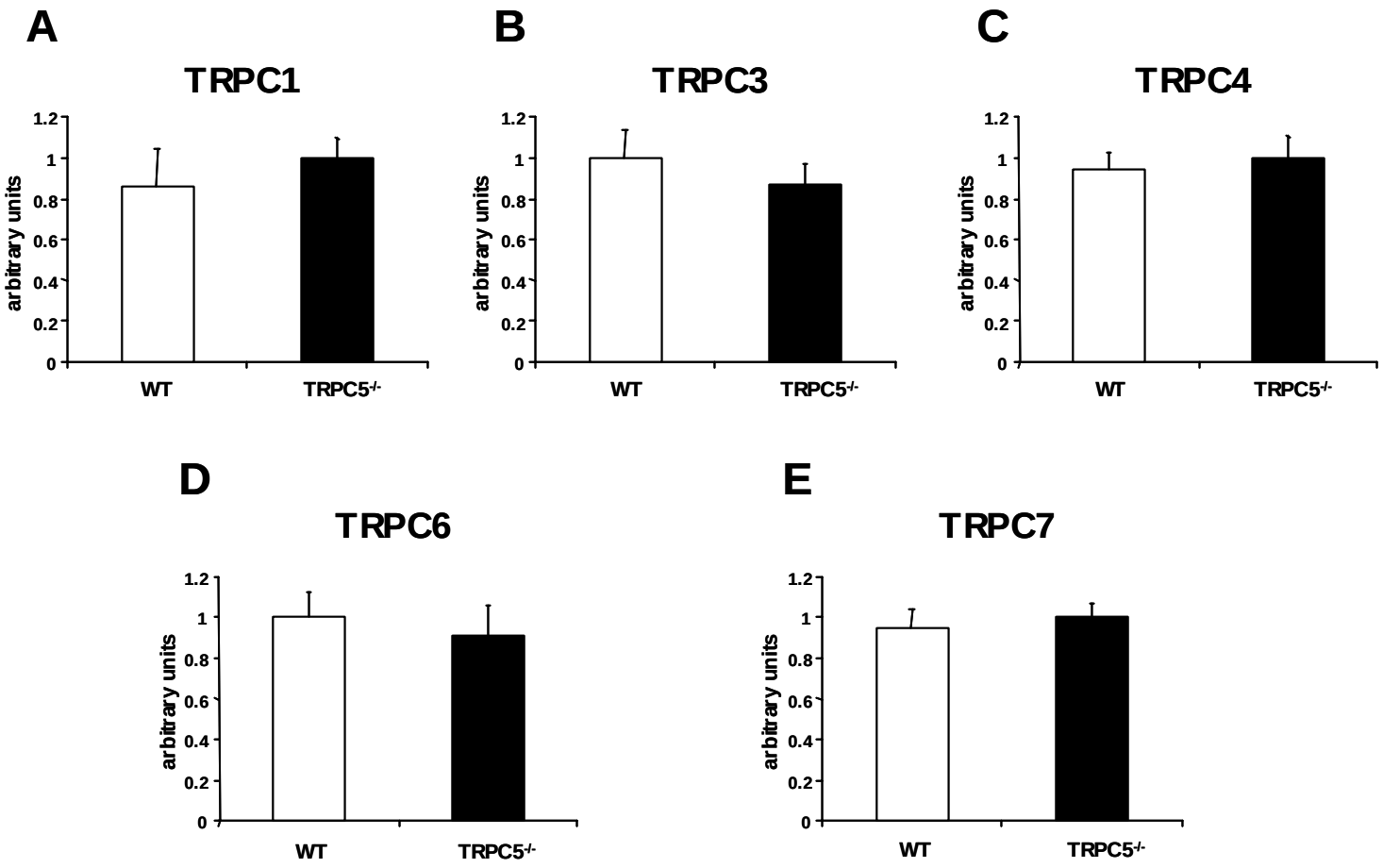

Supplementary Fig.4
Riccio et al.

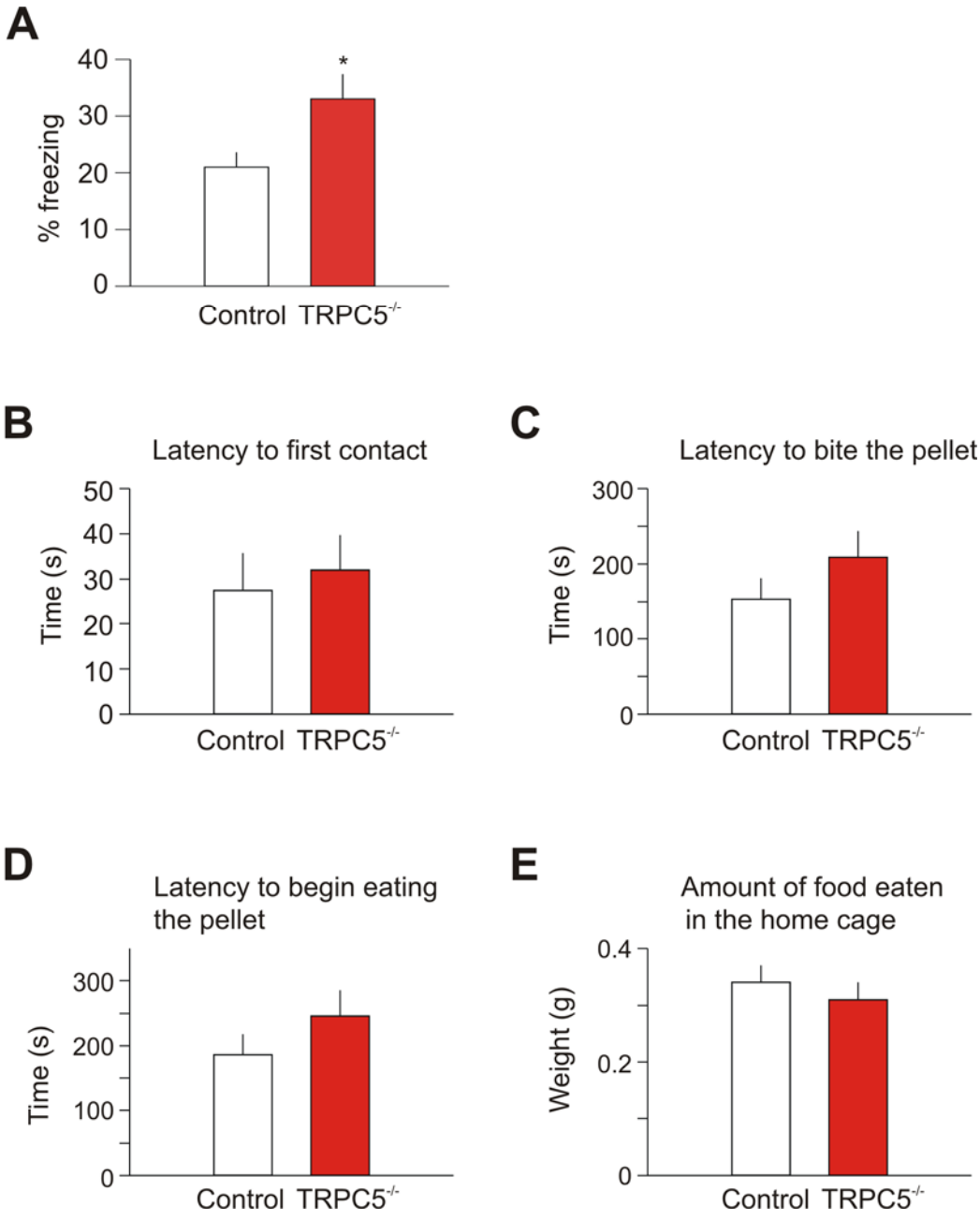

Supplementary Fig. 5
Riccio et al.

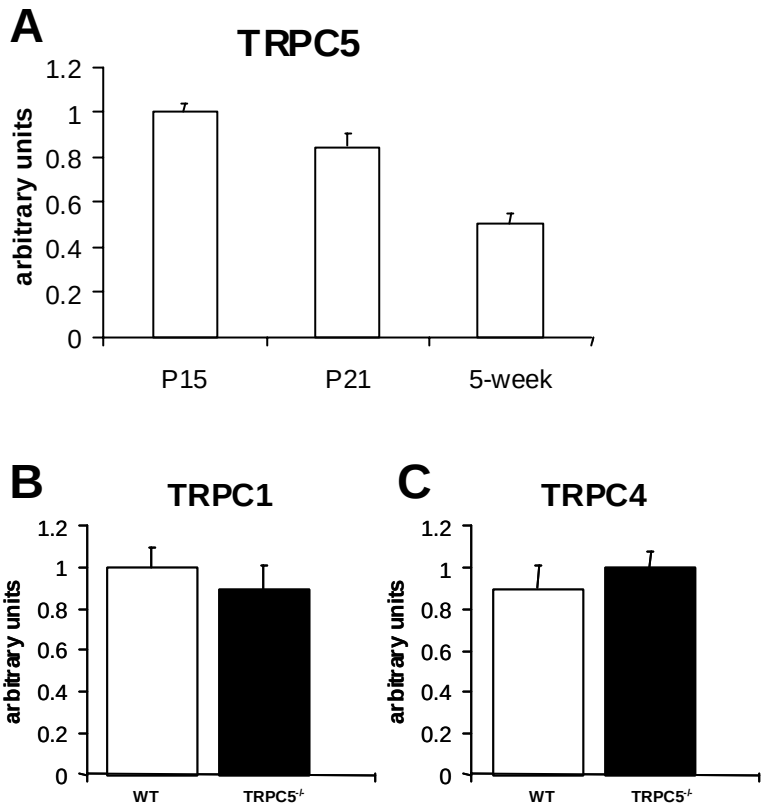

D

Oligonucleotide sequences

Gene	Accession number	Primer	Sequence 5'-3'
mTRPC1	NM_011643	F	TGCTCGCATACCTCGAAAGG
		R	CTCGTCTCTCTTTTGCTTCAAGTTT
mTRPC3	NM_019510	F	TCAATCAGCCAACACGATATCAG
		R	CTTCATTCACCTCATCGTTTTCTTT
mTRPC4	NM_016984	F	TCAGCCTCTTTGATTTAACCACTCT
		R	TGTCTCTCGGAGGCAATGG
mTRPC5	NM_009428	F	TGCGGTCGGGTGCTTTAA
		R	TGGCACCTGGAGCTTCAAG
mTRPC6	NM_053559	F	CAATATCAGAAAATCATGAAGAGACTCA
		R	TTCACCTCATCGCTCTCCTTATC
mTRPC7	NM_012035	F	GAAGCGGCTCATAAAGAGATACG
		R	TGAGTTCACCTTCATTGACTTCATC
mActin	NM_007393	F	GCTCTGGCTCCTAGCACCAT
		R	GCCACCGATCCACACAGAGT

Supplementary Fig. 6
Riccio et al.

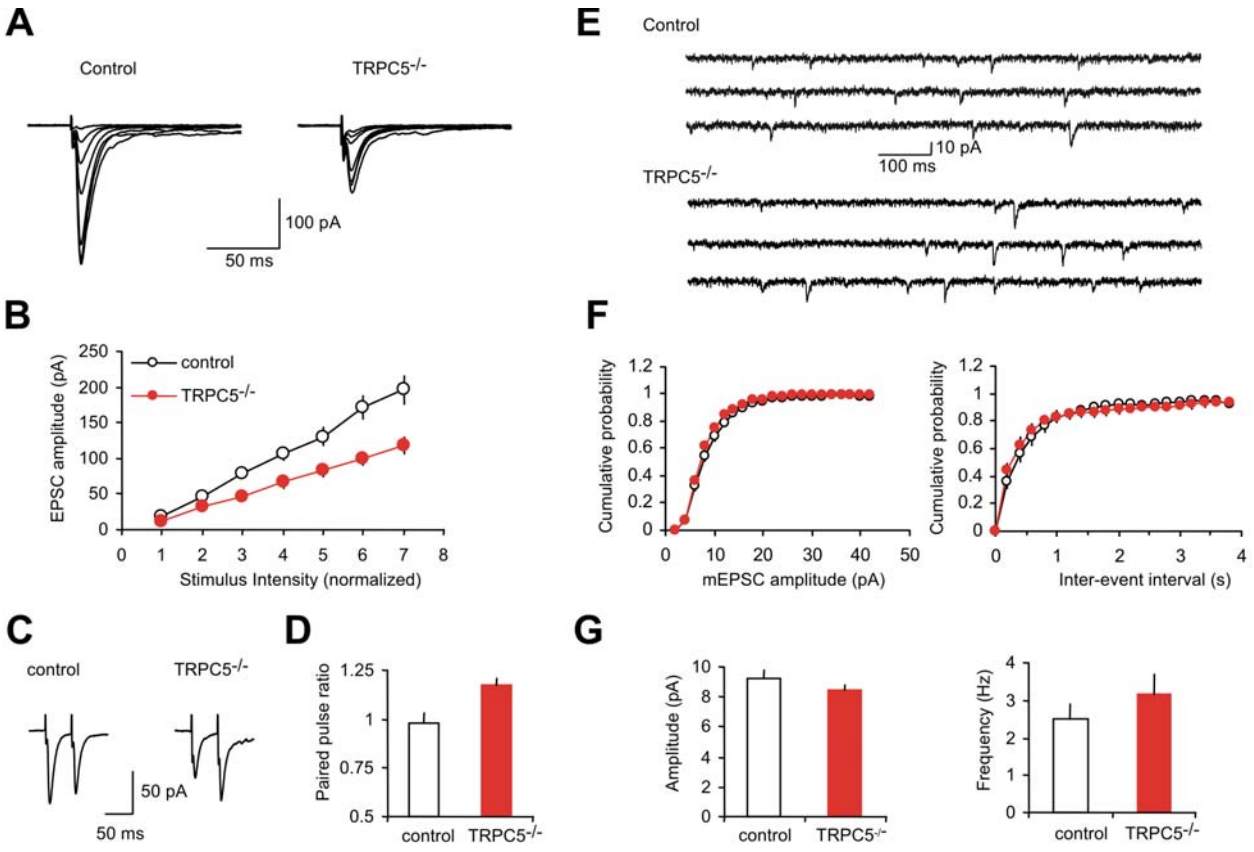

Supplementary Fig. 7
Riccio et al.

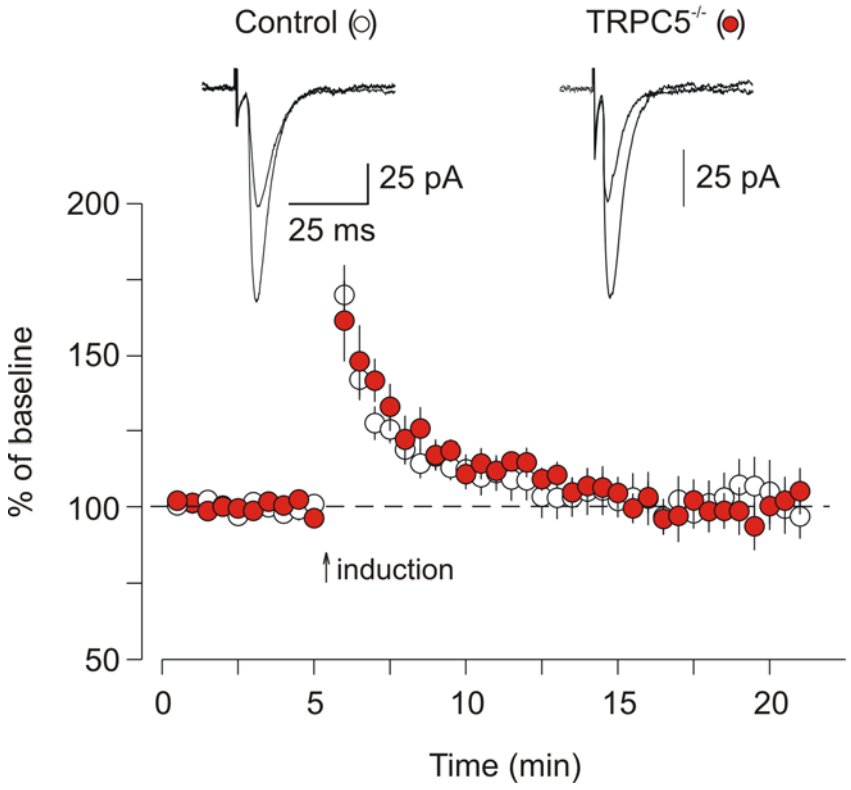

Supplementary Fig. 8
Riccio et al.

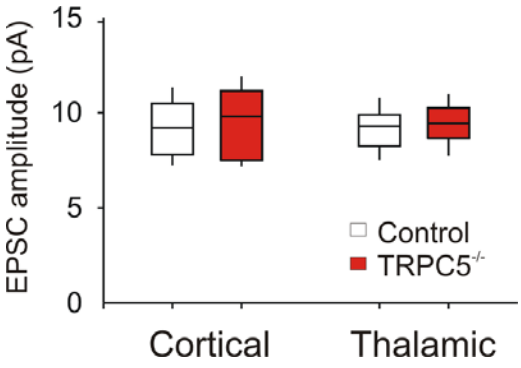

Supplementary Fig. 9
Riccio et al.

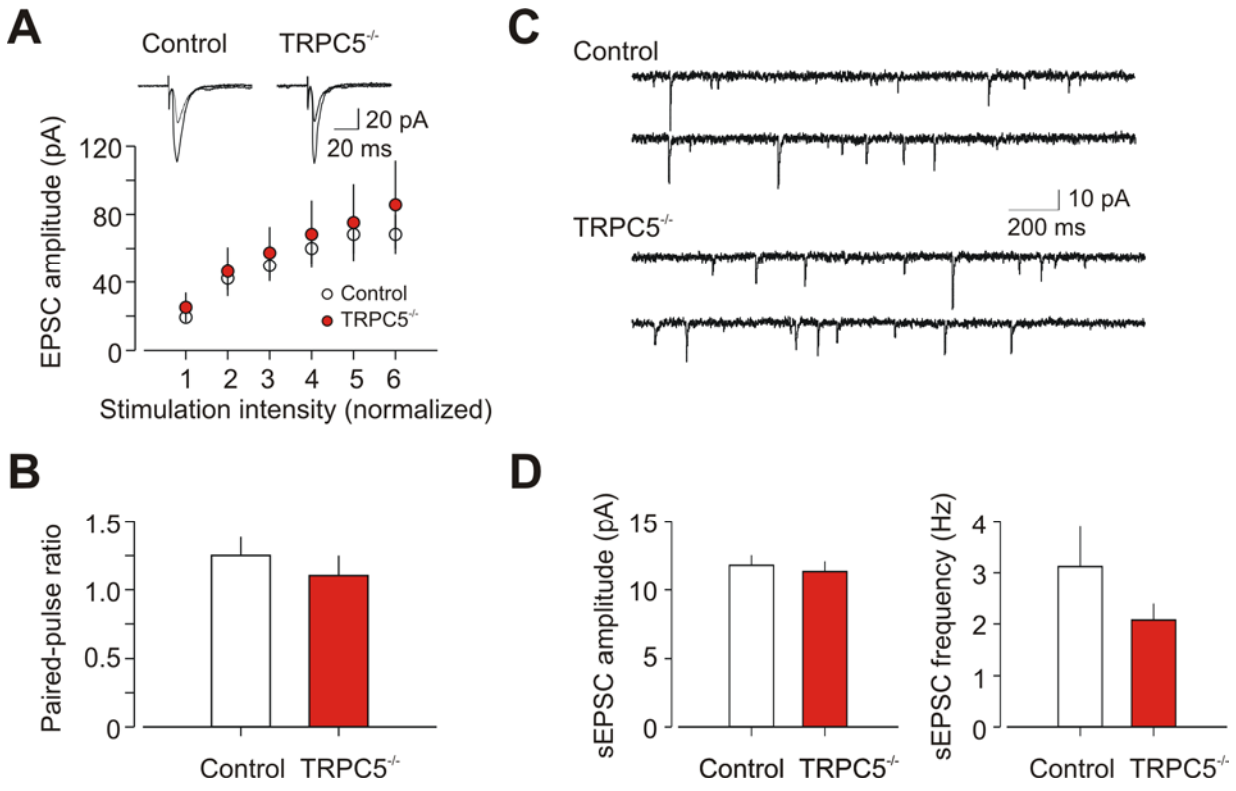

Supplementary Fig. 10
Riccio et al.